Excitation of the $1s_5$, $1s_4$, $1s_3$, and $1s_2$ levels of argon by low-energy electrons

K. Tachibana
Department of Electronics, Kyoto Institute of Technology, Matsugasaki, Sakyo-ku, Kyoto 606 Japan
(Received 13 March 1986)

Excitation rate coefficients for the $1s_5$, $1s_4$, $1s_3$, and $1s_2$ levels of argon by collisions with low-energy electrons have been measured using a drift-tube technique. Time dependences of the absolute population densities of the excited levels were measured by an absorption method with a tunable diode laser as a light source. The absorption data were analyzed according to the rate equations for these levels and the excitation rate coefficient per unit length of electron drift and per argon-atom density was obtained for each level as a function of the electric field to gas density ratio E/N. The values for the $1s_5$ level vary from 2.0×10^{-19} to 2.5×10^{-17} cm^2 as E/N increases from 5×10^{-17} to 5×10^{-15} V cm^2. In comparison with these values, those for the $1s_3$ level are about one-fifth, those for the $1s_4$ level are about the same, and those for the $1s_2$ level are slightly larger in respective measured E/N ranges. In order to estimate the cascading effects from the higher-lying levels, excitation rate coefficients for the $2p$ and $3p$ levels have also been measured from absolute intensities of the line emissions. From a comparison of all the measured values of the excitation rate coefficients with those calculated from the Boltzmann analysis, a recommended set of cross sections for these levels has been deduced.

I. INTRODUCTION

The lowest excited states of rare-gas atoms have important roles in various kinds of gas discharges because of their high stored energy and high population densities in the plasmas. The formation of excimers in rare-gas halide lasers[1] and the dissociation of parent gas molecules by excitation transfer in various plasmas used in semiconductor processings such as the plasma chemical vapor deposition of thin films[2] are listed as examples of the roles they play in recent topical applications. Therefore, precise knowledge of the cross sections and/or the rate coefficients for excitation of these states by electron collisions is required for the modeling of these discharges. This reason has motivated many recent experiments for the measurements of the cross sections for excitation of the individual sublevels within the lowest excited electronic states of neon,[3] argon,[4] and krypton.[5] However, there is no precise measurement as yet, to our knowledge, of the excitation rate coefficients for the $1s_5$, $1s_4$, $1s_3$, and $1s_2$ levels (Paschen notation is used throughout this paper) of those rare gases except for some recent reports on the total metastable excitation of argon.[6–8]

The principal objective of this paper is to present the first direct measurement of the individual excitation rate coefficients for the lowest metastable states ($1s_5$ and $1s_3$) and the lowest resonance states ($1s_4$ and $1s_2$) of argon using a drift-tube technique. The excitation rate coefficients, on the other hand, can be calculated from the corresponding cross sections through the Boltzmann-equation analysis, if a complete set of cross sections for the momentum transfer, the excitations, and the ionization is provided. Therefore, as the second objective of this paper, a comparison of the measured rate coefficients with the calculation using previously reported cross sections is performed and a recommended set of the cross sections for argon is presented.

The principle of the experiment is based on the absolute measurement of population densities of the excited atoms produced by collisions with slow electrons drifting under an applied electric field. The measurement has become possible using a very sensitive absorption technique with a frequency-stabilized single-mode laser as a light source, since the densities to be measured are of the order 10^{4-8} cm^{-3}. This experiment supplies the effective rate coefficients which include not only the direct excitations but also the cascade contributions from higher-lying levels. In order to estimate the cascade effects, the excitation rate coefficients for the $2p$ and $3p$ levels have also been measured. The experimental setup and procedure are described in Sec. II and the relevant theory for the data analysis is described in Sec. III. Experimental results are given in Sec. IV. A comparison of the experimental results with those calculated from the Boltzmann analysis is given in Sec. V and absolute values of the cross sections for the $1s$ levels near the threshold are determined.

II. EXPERIMENTAL APPARATUS AND PROCEDURE

The experimental setup is shown schematically in Fig. 1. The drift tube is the same one used for the measurement of the excitation rate coefficient for the $2p$ levels of neon[9] and described there in detail. The tube has two parallel electrodes of 15 cm diameter which have been shaped according to the calculation of Harrison[10] for keeping the applied electric field uniform. The electrode separation was 3 cm. One of the electrodes was equipped with a Au-Pd photocathode of 4.8 cm diameter and illuminated from the back by a deuterium lamp. Typical emission current was 0.2 μA in vacuum. The drift tube was evacuated down to 10^{-4} Pa by a diffusion pump be-

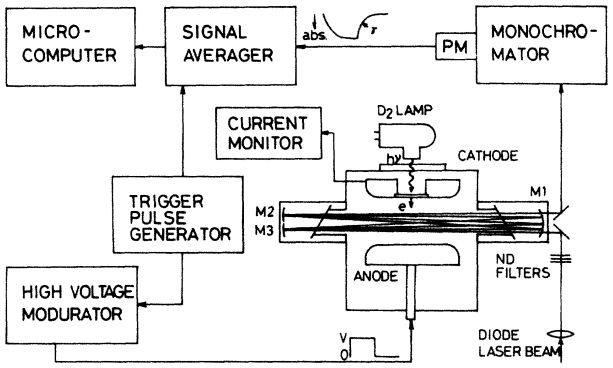

FIG. 1. Schematic diagram of the experimental setup.

fore each run. The outgassing rate was less than 10^{-3} Pa/min. Research-grade argon gas of 99.999% nominal purity was used without further purification. The gas pressure used in the measurement was 10—2000 Pa. A square-wave accelerating voltage of 50—400 V was applied between the electrodes, the period of which was varied from 10 to 100 msec according to the length of rise and fall of the absorption signal, which depended on the filling gas pressure, so as to allow the population density to reach the quasisteady state and then to decay to zero. The values of the ratio of the electric field to the gas density E/N studied in the present work ranged from 5×10^{-17} to 5×10^{-15} V cm^2, corresponding to electron mean energy from 5 to 10 eV estimated by the Boltzmann analysis described in Sec. V.

The light source used for the absorption measurement is a $Ga_{1-x}Al_xAs$ diode laser which is similar to that used in a previous measurement of the line profiles,[11] but its spectral shape has no fine structures and its linewidth is less than a few tens of MHz. The frequency of the laser was locked to the center of the absorption line of argon with a standard feedback technique[12] using the first derivative of the absorption line profile as a feedback signal to the injection current. The fluctuation of the frequency was monitored by absorption through a reference discharge tube and estimated to be less than 100 MHz. Practically, if the temperature of the laser was stabilized to 10^{-4} K, the feedback stabilization by injection current was not necessary for a typical measuring time of 1—10 min. The spectral lines used for measurement of the population densities of $1s_5$, $1s_4$, $1s_3$, and $1s_2$ levels were 811.5, 810.4, 794.8, and 840.8 nm, respectively. Three different diode lasers were used to cover these spectra.

A multiple-pass configuration (essentially a White cell[13]) used in the absorption measurement was composed of a concave mirror of 80 cm radius of curvature, which has two notches for the entrance and the exit of the laser beam, and two mirrors of the same curvature at the other side of the drift tube. The number of passes was 24, which corresponded to an absorption length of 115 cm in the drift region. The laser beam was folded parallel to the plane of the electrode surface and was set to pass through the center of the two electrodes. The laser beam was attenuated by a combination of neutral-density filters in front of the entrance mirror. The beam diameter in the drift region was about 1 mm and the power density there was about a few μW/mm^2. This power level was low enough to avoid the disturbance in the population densities caused by the pumping effect by the probing laser beam.

The absorption signal was detected by a photomultiplier through a monochromator of 50 cm focal length and fed to a digitizer-averager system by which the signal was cumulatively averaged for 100—10 000 times and then sent to a microcomputer for analysis of the waveform. Typical values of the absorption at the peak ranged from 0.02% to 20% for the metastable levels and 0.01% to 0.2% for the resonance levels. The excited-atom density was deduced using the literature value of the transition probability,[14] taking into account the effect of the pressure broadening and shift of the absorption line profile which we had reported previously.[11] The detection limit (noise-equivalent density) of the present system was about 10^4 cm^{-3}.

III. THEORY OF THE EXPERIMENT

The theory for the data analysis in the present experiment is similar to that for the experiments on O_2 by Lawton and Phelps[15] for the $b\,^1\Sigma_g^+$ state and by Tachibana and Phelps[16] for the $a\,^1\Delta_g$ state. In the present case for argon, however, we have two different situations; there are four sublevels within the lowest excited electronic configuration and the excited-state densities are derived from the absorption measurement instead of the absolute emission intensity measurement. A brief description of the theory is given in the following.

The time and spatial dependence of the electron density $n_e(z,t)$ is given by

$$\frac{\partial n_e}{\partial t}+w_e\frac{\partial n_e}{\partial z}=k_iNn_e\ , \tag{1}$$

where z is the axial position measured from the cathode, N is the argon-atom density in the ground state, w_e is the electron drift velocity, and k_i is the ionization rate constant. The population densities of the metastable level ($1s_5$ or $1s_3$) $M(z,t)$ and the resonance level ($1s_4$ or $1s_2$) $R(z,t)$ are given by the following equations, respectively, when the collisional population mixing within the sublevels is neglected (the validity of this assumption will be discussed later in Sec. VI):

$$\frac{\partial M}{\partial t}=k_Mn_eN+D\frac{\partial^2M}{\partial z^2}-(K_1N+K_2N^2)M\ , \tag{2}$$

$$\frac{\partial R}{\partial t}=k_Rn_eN-\nu_IR\ , \tag{3}$$

where k_M and k_R are the respective rate constants of the metastable and the resonance levels for excitation from the ground state by collisions with electrons, K_1 and K_2 are the rate constants of the metastable level for depopulations, respectively, by the two-body and the three-body collisions with ground-state atoms, D is the diffusion constant for the metastable atoms, and ν_I is the effective transition probability for the resonance level in which the

radiation trapping effect is taken into account. The radial diffusion term was neglected in Eq. (2) according to the argument in Ref. 15. For the resonance level the collisional loss processes and the diffusion term were also neglected in comparison to the radiation loss under our experimental condition.

The solution of Eq. (1) at the steady state gives the axial electron density distribution

$$n_e(z)=n_e(0)e^{\alpha_i z}, \tag{4}$$

where $\alpha_i \equiv k_i N/w_e$ and $n_e(0)$ is the electron density at the cathode surface ($z=0$). Substitution of this result into Eqs. (2) and (3) gives

$$M(z)=k_M N n_e(0)\sum_m (b_m/\gamma_m)\sin(m\pi z/L), \tag{5}$$

$$R(z)=k_R N n_e(0)e^{\alpha_i z}/\nu_I, \tag{6}$$

where $m \geq 1$, L is the electrode separation, and γ_m and b_m are given, respectively, by

$$\gamma_m = D(m\pi/L)^2 + K_1 N + K_2 N^2, \tag{7}$$

$$b_m = 2\pi m[1-e^{\alpha_i L}\cos(m\pi)]/[(\alpha_i L)^2+(m\pi)^2]. \tag{8}$$

From the absorption measurement we can determine the densities of the excited atoms at the center of the drift region; $M(z_0)$ and $R(z_0)$, where $z_0=L/2$. Using the following relations[15] between the electron current leaving the cathode surface i_c, the total current detected in the external circuit i, and its electron component i_e,

$$i_c = eAn_e(0)w_e, \tag{9}$$

$$i_e = i_c(e^{\alpha_i L}-1)/\alpha_i L, \tag{10}$$

$$i/i_e \equiv q = \alpha_i L e^{\alpha_i L}/(e^{\alpha_i L}-1), \tag{11}$$

where A is the area of the drift region (assumed to be equal to the photocathode area), we can substitute $n_e(0)$ with the directly measurable quantity i in Eqs. (5) and (6). Then the excitation rate coefficients for the metastable levels and the resonance levels are given, respectively, by

$$\alpha_M/N \equiv \frac{k_M}{w_e} = \frac{M(z_0)\gamma_1}{N(i/qeA)G\beta}, \tag{12}$$

$$\alpha_R/N \equiv \frac{k_R}{w_e} = \frac{R(z_0)\nu_I}{N(i/qeA)\beta}. \tag{13}$$

Here we have defined the geometrical factors G and β for the spatial distribution of the metastable atoms and for that of the electron current, respectively, as

$$G = (\gamma_1/e^{\alpha_i z_0})\sum_m (b_m/\gamma_m)\sin(m\pi/2), \tag{14}$$

$$\beta = \alpha_i L e^{\alpha_i z_0}/(e^{\alpha_i L}-1). \tag{15}$$

These factors appear because we are measuring the excited-atom densities only in the limited region of the drift space.

The value for γ_1 in Eq. (12) is determined from the time-dependent solution of the metastable density $M(z,t)$. The second term of Eq. (2) can be substituted by $-D_0/(\Lambda^2 N)M$, where $D_0=DN$ and $\Lambda=L/\pi$, if the diffusion in the fundamental mode is dominant; equivalent to the assumption that the production of the metastable atoms is uniform along z when $\alpha_i L \ll 1$. (Under the assumption the spatial distribution of M is always given by the zeroth-order Bessel function.) Then the time dependence of M is given by $M_0[1-\exp(-\gamma_1 t)]$ and $M_0\exp(-\gamma_1 t)$, respectively, in the rise and the fall periods of the accelerating voltage, where M_0 is the density at the quasisteady state. When the assumption fails at the higher E/N range, the time behavior of M cannot be represented by single-exponential functions. However, the decay rate of M in the late part of the fall period still gives γ_1.[17] In that case, therefore, the waveform only in the fall period is used in the analysis. (It is also noted that, if the density of the metastable atoms produced in the drift region becomes high, the waveform in the rise period is distorted due to the secondary electron current induced by their attack upon the cathode surface.[18]) On the other hand, the value of ν_I was not able to be measured directly because the signal was too small to analyze the waveform due to the small population densities of the resonance levels and also because the radiative decay rate was beyond the time response of the present measuring system. Therefore, we have calculated the values of ν_I by the following equation:[19,20]

$$\nu_I = 0.22(\lambda/L)^{1/2}/\tau_U, \tag{16}$$

where λ is the wavelength of the resonance line and τ_U is the radiative lifetime for the resonance level, for which the literature values[21] were used. The values of ν_I for the $1s_4$ and $1s_2$ levels were 4.74×10^4 and 2.01×10^5 $\sec^{-1}$, respectively.

IV. EXPERIMENTAL RESULTS

A typical example of the absorption signal is given in Fig. 2, which has been taken at a relatively low signal level. The values of γ_1 obtained from such waveforms using a least-squares fitting are shown in Fig. 3 for the $1s_5$ and $1s_3$ levels. It is known from Eq. (7) that γ_1 are divided into three components: diffusion loss and the two-body and the three-body collision losses. These components are shown in the figure by solid and dashed straight lines for the $1s_5$ and $1s_3$ levels, respectively. The rate constants for these processes for the $1s_5$ level are determined as follows: $D_0=2.4\times10^{18}$ $\mathrm{cm}^{-1}\sec^{-1}$, $K_1=2.3\times10^{-15}$ $\mathrm{cm}^3\sec^{-1}$, and $K_2=1.4\times10^{-32}$ $\mathrm{cm}^6\sec^{-1}$. For the $1s_3$ level these values become $D_0=2.4\times10^{18}$ $\mathrm{cm}^{-1}\sec^{-1}$, $K_1=4.3\times10^{-15}$ $\mathrm{cm}^3\sec^{-1}$, and $K_2=1.5\times10^{-32}$ $\mathrm{cm}^6\sec^{-1}$. When we compare these with previously reported values tabulated in Ref. 22, the present values for K_2 are larger than the reported values by a factor 1.3–2. The reason for the difference will be discussed in Sec. VI.

The values of the excitation rate coefficient α_M/N for the $1s_5$ and $1s_3$ levels obtained from Eq. (12) are shown in Fig. 4 as a function of E/N. The values of α_R/N for the $1s_4$ and $1s_2$ levels obtained from Eq. (13) are shown in Fig. 5. The solid curves in these figures represent the values for the direct excitation from the ground state which are calculated by the Boltzmann analysis as will be described in Sec. V. The measured values fit well to the

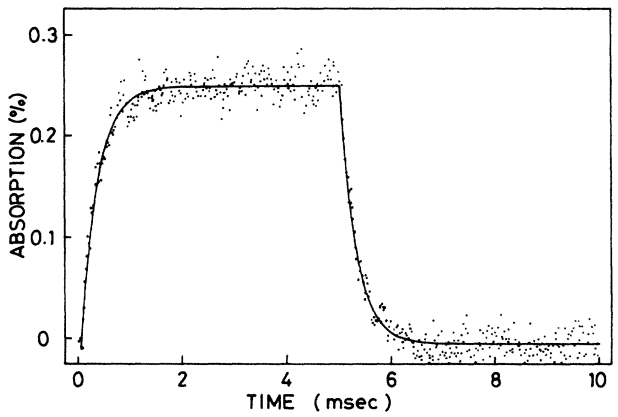

FIG. 2. An example of waveform of the absorption signal for the $1s_5$ level at $E/N=1\times10^{-16}$ V cm^2, $N=3.2\times10^{17}$ cm^{-3}. Solid curve shows the least-squares fitting to the exponential rise and fall. Maximum absorption corresponds to a density of 1.5×10^6 cm^{-3}.

calculation at lower values of E/N, but these become larger than the calculation as E/N increases. This difference can be attributed to the cascade population of the $1s$ levels from the higher-lying levels.

In order to estimate the cascade contribution, we have measured the excitation rate coefficients for the $2p$ and $3p$ levels which have the main contributions to $1s$ levels. The experiment was performed by measuring the absolute intensities of the line emissions from these levels to $1s$ levels in a manner similar to the one which we had reported previously for the $2p$ levels of neon.[9] In Table I are given the obtained values for the optical rate coefficient α_{ij}/N for

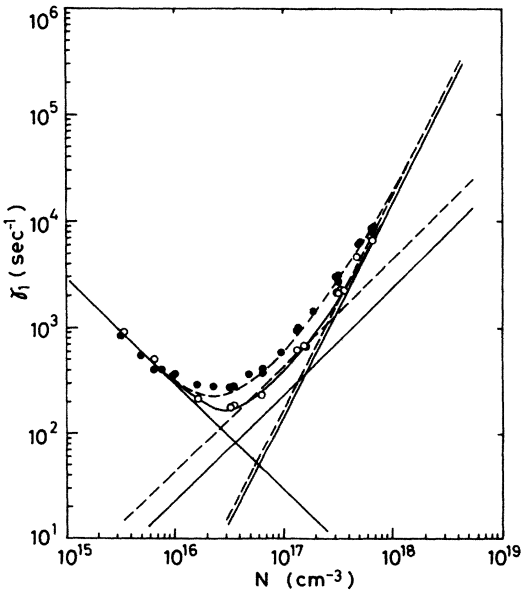

FIG. 3. Dependence of the decay rate for the $1s_5$ (○) and $1s_3$ (●) levels on the gas density N. See text for the fitted lines.

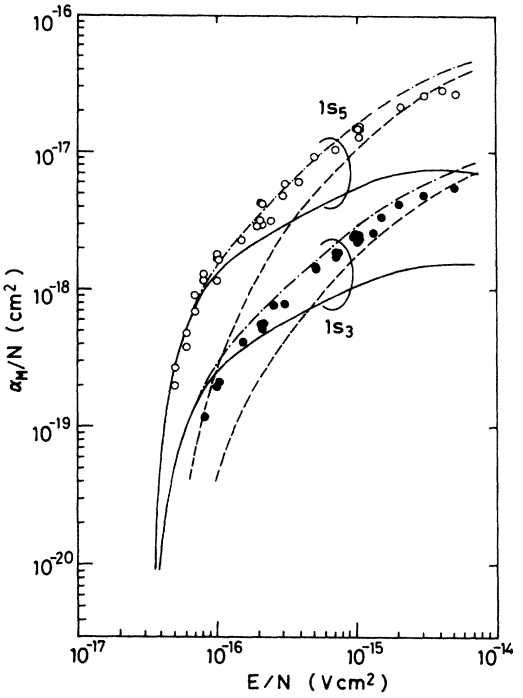

FIG. 4. Excitation rate coefficient α_M/N for the $1s_5$ (○) and $1s_3$ (●) levels as a function of E/N. Solid curve shows the values for the direct excitation calculated from Boltzmann analysis, dashed curve shows the estimated cascade contribution, and dot-dashed curve shows the sum of them.

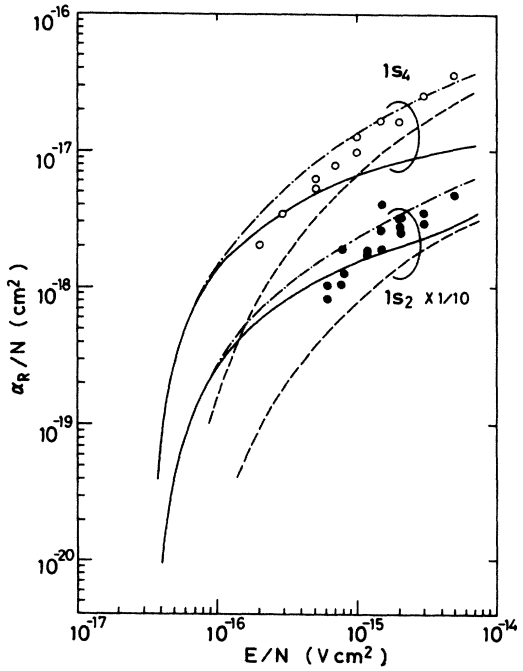

FIG. 5. Excitation rate coefficient α_R/N for the $1s_4$ (○) and $1s_2$ (●) levels as a function of E/N. The values for the $1s_2$ level are reduced by a factor 10. Meanings of the curves are the same as in Fig. 4.

TABLE I. Optical excitation rate coefficient α_{ij}/N for the $2p_i$-$1s_j$ transition measured at $E/N=1\times10^{-15}$ V cm^2. For each transition the upper entry is the wavelength (nm), the middle one is the transition probability (10^8 sec) (Ref. 14), and the lowest one is the measured value of the rate coefficient normalized to α_{12}/N.

j \ i	$2p_1$	$2p_2$	$2p_3$	$2p_4$	$2p_5$	$2p_6$	$2p_7$	$2p_8$	$2p_9$	$2p_{10}$	$\sum_i^a$
$1s_2$	750.4	826.5	840.8	852.1		922.5	935.4	978.5		1148.8	
	0.472	0.168	0.244	0.147		0.059	0.012	0.016		0.0025	
	1	0.171	0.568	0.509		0.206	(0.014)	(0.053)		(0.008)	2.529
$1s_3$		772.4		794.8			866.8			1047.0	
		0.127		0.196			0.028			0.012	
		0.149		0.334			0.045			(0.042)	0.570
$1s_4$	667.7	727.3	738.4	747.1	751.5	800.6	810.4	842.5		965.8	
	0.0024	0.020	0.087	2.5×10^{-4}	0.430	0.047	0.277	0.233		0.060	
	0.010	0.001	0.306		0.538	0.200	0.241	0.640		(0.215)	2.151
$1s_5$		696.5	706.7	714.7		763.5	772.4	801.5	811.5	912.3	
		0.067	0.040	0.0065		0.274	0.057	0.096	0.366	0.212	
		0.136	0.118	0.039		0.738	0.075	0.363	1.180	0.760	3.409
$\sum_j^b$	1.010	0.457	0.992	0.882	0.538	1.144	0.375	1.056	1.180	1.025	8.659

[a]Relative cascade contribution to each $1s_j$ level.
[b]Relative level excitation rate coefficient for each $2p_i$ level.

the $2p_i$-$1s_j$ transition which includes the ratio of branching from the same upper level to the different lower levels. The values in the table have been measured at $E/N=1\times10^{-15}$ V cm^2 and normalized to the value for the $2p_1$-$1s_2$ (750.4-nm) transition. Since the measurement for the transitions of which the wavelengths are larger than 930 nm was not possible because of the sensitivity of the present system, the values for those transitions have been estimated from the literature values of the transition probabilities[14] and are shown in parentheses in the table. From this result it is seen that about 25—40 % of the total excitation of the $2p$ levels cascades to each of the $1s_5$, $1s_4$, and $1s_2$ levels, while the contribution to the $1s_3$ level is much smaller and only amounts to about 7% because the number of allowed transitions to the level is small. It is also known from the table that the total excitation rate coefficient for all of the $2p$ levels is given by multiplying a factor 8.7 to the value for the $2p_1$-$1s_2$ transition or 11.7 to the value for the $2p_6$-$1s_5$ transition. The rate coefficients for these two transitions and that for the total $2p$ levels obtained in such a manner are shown in Fig. 6 as functions of E/N. The solid curve in the figure represents the calculated values from the Boltzmann analysis. When the filling pressure becomes high, the collisional population mixing within the $2p$ levels may occur[23] and the ratios of the cascading contribution to each $1s$ level become dependent on the pressure. However, we assumed the ratios are independent of the pressure, because at higher E/N range, where the cascading contribution becomes large, most of the measurements have been carried out at relatively low pressure (<300 Pa), at which the problem can be avoided.[23] The fact that the values of α_{ij}/N for the two transitions shown in Fig. 6 do not have different functional dependences on E/N also supports the assumption.

As a typical example for the cascade transitions from the $3p$ levels, the values for the $3p_5$-$1s_4$ (419.8-nm) transition are also shown in Fig. 6. It is seen from this example that the cascade contributions from the $3p$ levels are smaller than those from the $2p$ levels by more than an order of magnitude and can be neglected in our experimen-

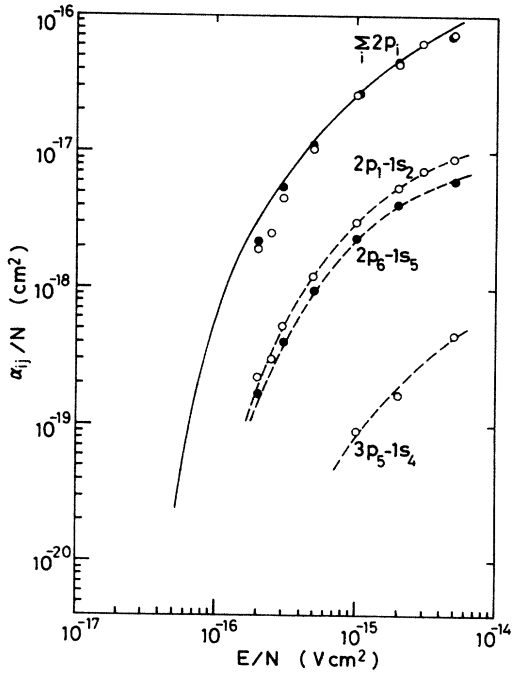

FIG. 6. Optical excitation rate coefficient α_{ij}/N for some of the $2p$ and $3p$ levels as a function of E/N. Dashed curve shows only the smoothly fitted one to the data. The total excitation rate coefficient for all of the $2p$ levels is also shown. Solid curve shows the values calculated from the Boltzmann analysis.

tal E/N range.

The cascade contributions for the individual $1s$ levels thus obtained are shown by the dashed curves in Figs. 4 and 5. The dot-dashed curves in those figures represent the effective excitation rate coefficient: the sum of the direct and the cascade excitations. The effective values then become in good agreement with the measured values over all the measured E/N ranges.

V. BOLTZMANN ANALYSIS

We have compared the measured values of the rate coefficients with those calculated by Boltzmann analysis in a conventional two-term expansion approximation[24] using the computer code of Luft.[25] The set of cross sections we have used in the Boltzmann analysis is shown in Fig. 7. The momentum transfer cross section is that recommended by Hayashi.[26] The ionization cross section is that measured by Rapp and Englander-Golden.[27] The absolute values of the cross sections for excitation of the four $1s$ levels have been carefully determined here from comparison of the calculation with the measurement using the shape of the relative cross sections measured by Pichanick and Simpson[28] and Brunt *et al.*[29] at electron energy ε from the threshold to 14 eV and the absolute values of Chujian and Cartwright[4] at ε larger than 16 eV. The cross section designated A refers to the total excitation cross section for all the higher-lying s and d states and that designated F refers to the total cross section for all of the other states (mostly the $2p$ state). The values for these two cross sections are taken from the report of Eggarter[30] and corrected slightly for the higher energy region using the total excitation cross section given by de Heer *et al.*[31]

The values of the rate coefficients calculated from the Boltzmann analysis with the present set of cross sections agree very well with the measured values as described above. Other calculated swarm parameters such as the drift velocity and the diffusion coefficient also agree well with literature values.[32] As for the ionization coefficient α_i/N, however, the calculated values become slightly larger than the values reported by Kruithof[33] at higher values of E/N as shown in Fig. 8. This difference may be due to the fact that in the Boltzmann analysis described above the effect of the secondary electrons produced in the drift region has not been considered. If we use a Boltzmann code in which this effect is taken into account,[34] the values of the calculated α_i/N become smaller at higher E/N and fit the measured values fairly well as shown by solid circles in the figure. The calculated values of the excitation rate coefficients for the $1s$ and $2p$ levels also become smaller than before by about 10—40% as E/N increases from 1×10^{-15} to 5×10^{-15} V cm^2 and the agreement with the measured values is improved.

VI. DISCUSSION

The most important problem in determining the direct excitation rate coefficients for the individual $1s$ levels is how to estimate or reduce the effect of the population mixing within the $1s$ levels by collisions with neutral atoms. This effect becomes important in the gas density region from 1×10^{16} to 3×10^{17} cm^{-3} as can be seen from

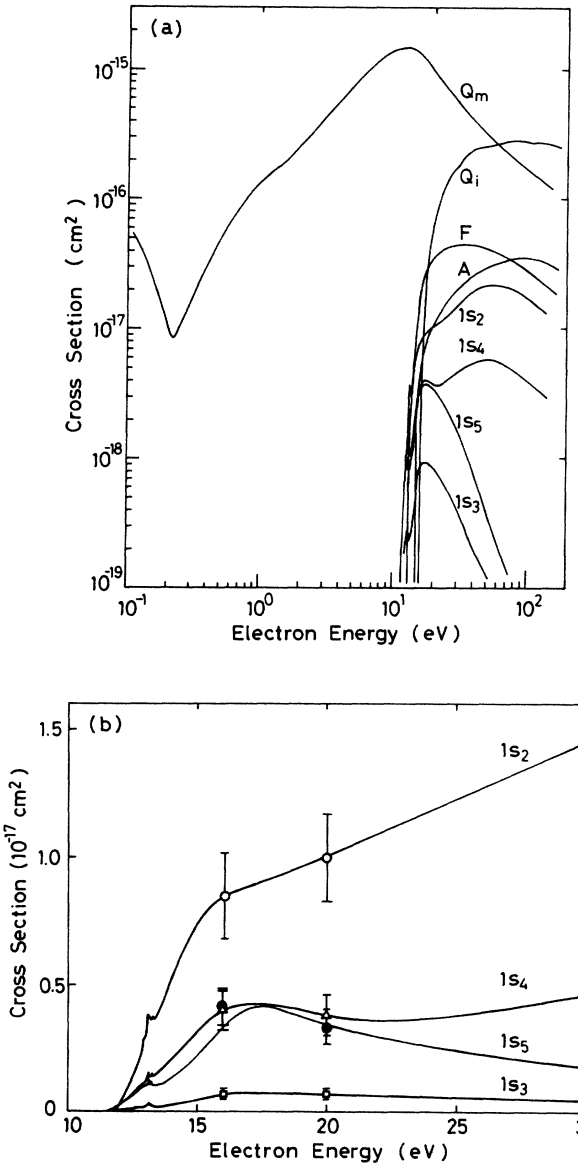

FIG. 7. (a) A set of cross sections for argon used in the Boltzmann analysis: Q_m, momentum transfer; Q_i, ionization; F, excitation of total forbidden levels; A, that of total allowed levels. (b) Part of the set for the four $1s$ levels. Data points represent the values of Chutjian and Cartwright (Ref. 4).

Fig. 3. At lower gas density the loss of the $1s_5$ and $1s_3$ atoms is mainly due to the diffusion to the electrodes and at higher gas density it is due to the three-body collisions leading mostly to the formation of excited molecules which decay by emission of vacuum-ultraviolet photons.[35] For the $1s_5$ level the mixing effect seems to be large because the energy of this level is the lowest and the rate constants for excitation transfer from the other $1s$ levels are expected to be larger compared to the reverse process at a gas temperature of 300 K. However, the population densities of the $1s_4$ and $1s_2$ levels are smaller than the metastable levels by more than 2 orders of magnitude be-

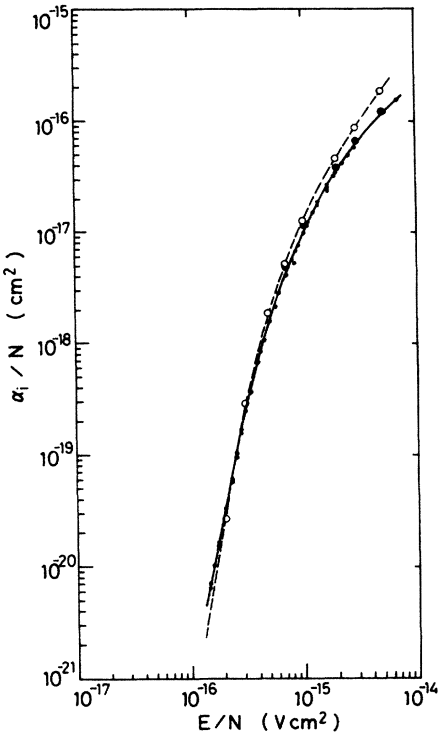

FIG. 8. Comparison of the calculated ionization rate coefficient α_i/N with measurement of Kruithof (solid curve, Ref. 33). ● and ○ are the values calculated with and without the effect of the secondary electrons, respectively.

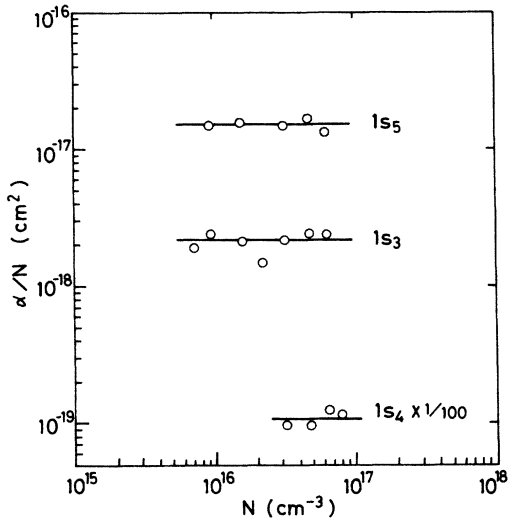

FIG. 9. Dependence of the excitation rate coefficient α/N for the $1s$ levels on the gas density N at a fixed value of $E/N = 1\times10^{-15}$ V cm^2.

cause of their fast radiative decay rate, so that transfer from these levels are negligible. Transfer from the $1s_3$ level, however, may not be negligible even though the population density of the level is about one-fifth of the density of the $1s_5$ level. Likewise, for the $1s_3$ level, transfer from the $1s_5$ level may not be negligible even though the rate constant is smaller than that for the reverse process since the density of $1s_5$ level is large. As for the $1s_4$ level, transfer from both the adjacent levels $1s_5$ and $1s_3$ is possible. For the $1s_2$ level, however, the effect seems to be small because this level lies higher than the other levels and the nearest $1s_3$ level has relatively small population density.

Anyway, we have to estimate the collisional mixing effect quantitatively by experiments. For this purpose we have measured the excitation rate coefficients at a typical E/N value of 1×10^{-15} V cm^2 at several values of the gas density. As shown in Fig. 9, any dependence of the rate coefficients on the gas density is not seen for the $1s_5$ and $1s_3$ levels within the experimental scatter. The most probable reason for this result may be that the purity of the argon gas used in the present experiment has not been high enough. If so, the measured rate constant for the two-body collisions, which is the source of the excitation transfer within the $1s$ levels, actually includes the contribution of the collision with the impurity atoms or molecules. Therefore, the apparent rate constant must become larger than the previously reported values as described in Sec. IV. Possible candidates for the impurity contained in the gas are N_2 and much smaller amounts of O_2 and H_2O. If these are the collision partners, the deactivation rate constant for the $1s$ levels is expected to be 10^{-11}–10^{-10} cm^3 sec^{-1},[36] so that an impurity concentration of only about 10 ppm can give a decay rate equivalent to that by neutral argon atoms. However, for the impurities such as N_2, the excited argon atoms transfer the energy to them, which then lose the energy by radiation. Therefore, it does not lead to the excitation transfer within the $1s$ levels but rather reduces the present problem. In fact, when we left the chamber for a long period after filling it with the argon gas and then measured the excitation rate coefficients, the values of γ_1 increased but the obtained values of the rate coefficient did not change even though γ_1 changed by a factor of 2–5. Fortunately, for argon the Penning ionization with such impurities does not occur and produces no further problems.

As for the $1s_4$ and $1s_2$ levels, the dependence of the rate coefficient on the gas density was measured only in a small E/N range as shown in Fig. 9 due to smallness of the signal, so that the same conclusion as above cannot be drawn for these two levels. However, as a rough estimation, suppose that the measurement is done at $N = 3\times10^{16}$ cm^{-3}, then about half of the population of the $1s_5$ and $1s_3$ levels may be transferred to the $1s_4$ level, leading to overestimation of α_R/N by about 50%. When the impurities are contained in the gas, this effect must be smaller. Anyway, in order to avoid the mixing effect, we have taken most of the data for these levels at lower or higher gas density where the effect can be reduced as stated above.

The other possible sources of errors in the determination of the excitation rate coefficients are as follows. The uncertainty in the determination of the value of γ_1 for the metastable levels by least-squares fitting (±5%). The un-

certainty of ν_I for the resonance levels ($\pm 10\%$), which is estimated from a comparison of the calculated values with those measured by Payne *et al.*[37] in a cylindrical geometry. The uncertainty in the derivation of the population density, which is included in the literature value of the transition probability ($\pm 10\%$) and in the absorption measurement due to the frequency fluctuation of the laser (0 to -5%). The uncertainties in the measurement of the current i ($\pm 5\%$) and the gas density ($\pm 5\%$). Therefore, the overall uncertainties included in the obtained values of the rate coefficients are $\pm 25\%$ and $\pm 30\%$ for the metastable levels and for the resonance levels, respectively, in which the uncertainties due to the modeling through the geometrical factors ($\pm 10\%$) are also included.

Since there are no data at present with which we can compare the present results of the excitation rate coefficients for the individual $1s$ levels, we compare here our result on the total metastable ($1s_5+1s_3$) excitation rate coefficient α_M^t/N with some previously reported results.[6–8] Figure 10 shows the comparison as a function of E/N. The present result agrees with those of Burgmans and Smeets[7] and Božin *et al.*[8] However, compared to the present direct method, the metastable atom density has been obtained in their measurements indirectly; from the current growth produced by Penning ionization of Hg atoms by metastable argon atoms and from the sensitized fluorescence emitted by N_2 molecules mixed in argon in small amounts, respectively. The values of Ferreira and Ricard[6] have a functional dependence different from that of the other data. Possibly this may be due to the uncertainty which is included in the determination of E/N since their measurement has been done in a positive column of a glow discharge instead of the Townsend discharge used in the other measurements.

Ferreira and Loureiro[38] have also deduced a set of cross sections for argon from the Boltzmann analysis. When we calculate α_M^t/N using their cross-section set with the same computer code as used in the present work, the results for the direct and the effective excitations become as shown by the dashed curves in Fig. 10, where the results obtained with our cross-section set are shown by the solid curves. It is seen from the comparison that the former values are larger than the latter, especially at the lower E/N region, and do not fit the present measured values. This is attributed to the difference in the values of the total metastable excitation cross section near the threshold. As for the ionization and the transport coefficients, however, both cross-section sets do not produce recognizable differences in the E/N region with which we are concerned.

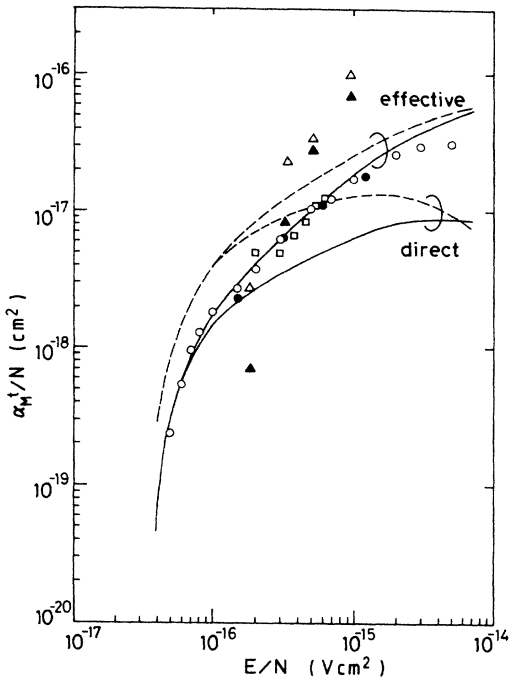

FIG. 10. Comparison of the total metastable excitation rate coefficient: △,▲, Ferreira and Ricard, Ref. 6; □, Božin *et al.*, Ref. 8; ●, Burgmans and Smeets, Ref. 7; ○, present work. See text for the curves.

ACKNOWLEDGMENTS

The author is indebted to Dr. Phelps of the Joint Institute for Laboratory Astrophysics, University of Colorado and National Bureau of Standards, who suggested this work. Thanks are also due to Dr. Teramoto and Dr. Shimizu of Matsusita Electronics, Inc. for support on the diode lasers used in the present experiment, to Professor Hayashi of Nagoya Institute of Technology for helpful discussions and allowing the author to use his computer code, and Professor Urano of Kyoto Institute of Technology for encouragement. This work is supported in part by a Grant-in-Aid for Scientific Research from the Ministry of Education, Science and Culture of Japan.

[1]See, e.g., *Excimer Lasers*, edited by C. K. Rhodes (Springer-Verlag, Berlin, 1979).

[2]See, e.g., *Hydrogenated Amorphous Silicon*, edited by J. I. Pankove (Academic, Orlando, 1984), Pt. A; Proceedings of the Eleventh International Conference on Amorphous and Liquid Semiconductors, Rome, 1985 [J. Non-Cryst. Solids **77&78**, 743 (1985)].

[3]M. H. Phillips, L. W. Anderson, and C. C. Lin, Phys. Rev. A **32**, 2117 (1985).

[4]A. Chutjian and D. C. Cartwright, Phys. Rev. A **23**, 2178 (1981).

[5]S. Trajmar, S. K. Srivastava, H. Tanaka, H. Nishimura, and D. C. Cartwright, Phys. Rev. A **23**, 2167 (1981).

[6]C. M. Ferreira and A. Ricard, J. Appl. Phys. **54**, 2261 (1983).

[7]A. L. J. Burgmans and A. H. M. Smeets, J. Phys. D **16**, 755 (1983).

[8]J. V. Božin, V. V. Urošević, and Z. Lj Petrović, Z. Phys. A **312**, 349 (1983).

[9]K. Tachibana, H. Harima, and Y. Urano, J. Phys. B **17**, 879 (1984).
[10]J. A. Harrison, Brit. J. Appl. Phys. **18**, 1617 (1967).
[11]K. Tachibana, H. Harima, and Y. Urano, J. Phys. B **15**, 3169 (1982).
[12]See, e.g., A. D. White, IEEE J. Quantum Electron. **QE-1**, 349 (1965); P. W. Smith, *ibid.* **QE-1**, 343 (1965).
[13]J. U. White, J. Opt. Soc. Am. **32**, 285 (1942).
[14]W. L. Wiese, M. W. Smith, and B. M. Miles, *Atomic Transition Probabilities* (U.S. Department of Commerce, Washington, D.C., 1969), Vol. 2.
[15]S. A. Lawton and A. V. Phelps, J. Chem. Phys. **69**, 1055 (1978).
[16]K. Tachibana and A. V. Phelps, J. Chem. Phys. **75**, 3315 (1981).
[17]A. V. Phelps and J. P. Molnar, Phys. Rev. **89**, 1202 (1953).
[18]J. P. Molnar, Phys. Rev. **83**, 933 (1951).
[19]A. V. Phelps, Phys. Rev. **114**, 1011 (1959).
[20]T. Holstein, Phys. Rev. **83**, 1159 (1951).
[21]G. M. Lawrence, Phys. Rev. A **175**, 40 (1968).
[22]J. H. Kolts and D. W. Setser, J. Chem. Phys. **68**, 4848 (1978).
[23]T. D. Nguyen and N. Sadeghi, Phys. Rev. A **18**, 1388 (1978).
[24]L. S. Frost and A. V. Phelps, Phys. Rev. **127**, 1621 (1962).
[25]P. E. Luft, Joint Institute for Laboratory Astrophysics (JILA) Information Center Report No. 14, 1975 (unpublished).
[26]M. Hayashi, Report of the Institute of Plasma Physics, Nagoya University, No. IPPJ-AM-19, 1981 (unpublished).
[27]D. Rapp and P. Englander-Golden, J. Chem. Phys. **43**, 1464 (1965).
[28]F. M. J. Pichanick and J. A. Simpson, Phys. Rev. **168**, 64 (1968).
[29]J. N. H. Brunt, G. C. King, and F. H. Read, J. Phys. B **9**, 2195 (1976); **10**, 3781 (1977).
[30]E. Eggarter, J. Chem. Phys. **62**, 833 (1975); E. Eggarter and M. Inokuti, Argonne National Laboratory Report No. ANL-80-58, 1980 (unpublished).
[31]F. J. de Heer, R. H. J. Jansen, and W. van der Kaay, J. Phys. B **12**, 979 (1979).
[32]See, e.g., J. Dutton, J. Phys. Chem. Ref. Data **4**, 577 (1975).
[33]A. A. Kruithof, Physica **7**, 519 (1944).
[34]M. Hayashi and T. Nimura, J. Appl. Phys. **54**, 4879 (1983).
[35]See, e.g., Y. Tanaka, W. C. Walker, and K. Yoshino, J. Chem. Phys. **70**, 380 (1979).
[36]See, e.g., L. G. Piper, J. E. Valazco, and D. W. Setser, J. Chem. Phys. **59**, 3323 (1973); J. de Calve and M. Bourene, *ibid.* **58**, 1446 (1973).
[37]M. G. Payne, J. E. Talmage, G. S. Hurst, and E. B. Wagner, Phys. Rev. A **9**, 1050 (1974).
[38]C. M. Ferreira and J. Loureiro, J. Phys. D **16**, 1611 (1983).